

UMGAD: Unsupervised Multiplex Graph Anomaly Detection

Xiang Li
Ocean University of China
Qingdao, China
lixiang1202@stu.ouc.edu.cn

Jianpeng Qi
Ocean University of China
Qingdao, China
qijianpeng@ouc.edu.cn

Zhongying Zhao
Shandong University of Science and
Technology
Qingdao, China
zyzhao@sdust.edu.cn

Guanjie Zheng
Shanghai Jiao Tong University
Shanghai, China
gjzheng@sjtu.edu.cn

Lei Cao
The University of Arizona
Tucson, AZ, USA
lcao@csail.mit.edu

Junyu Dong
Ocean University of China
Qingdao, China
dongjunyu@ouc.edu.cn

Yanwei Yu[†]
Ocean University of China
Qingdao, China
yuyanwei@ouc.edu.cn

Abstract

Graph anomaly detection (GAD) is a critical task in graph machine learning, with the primary objective of identifying anomalous nodes that deviate significantly from the majority. This task is widely applied in various real-world scenarios, including fraud detection and social network analysis. However, existing GAD methods still face two major challenges: (1) They are often limited to detecting anomalies in single-type interaction graphs and struggle with multiple interaction types in multiplex heterogeneous graphs; (2) In unsupervised scenarios, selecting appropriate anomaly score thresholds remains a significant challenge for accurate anomaly detection. To address the above challenges, we propose a novel Unsupervised Multiplex Graph Anomaly Detection method, named UMGAD. We first learn multi-relational correlations among nodes in multiplex heterogeneous graphs and capture anomaly information during node attribute and structure reconstruction through graph-masked autoencoder (GMAE). Then, to further weaken the influence of noise and redundant information on abnormal information extraction, we generate attribute-level and subgraph-level augmented-view graphs respectively, and perform attribute and structure reconstruction through GMAE. Finally, We learn to optimize node attributes and structural features through contrastive learning between original-view and augmented-view graphs to improve the model's ability to capture anomalies. Meanwhile, we also propose a new anomaly score threshold selection strategy, which allows the model to be independent of the ground truth in real unsupervised scenarios. Extensive experiments on four datasets

show that our UMGAD significantly outperforms state-of-the-art methods, achieving average improvements of 13.48% in AUC and 11.68% in Macro-F1 across all datasets. The source code of our model is available at <https://anonymous.4open.science/r/UMGAD-1F3B>.

CCS Concepts

• **Mathematics of computing** → *Graph algorithms*; • **Computing methodologies** → *Learning latent representations*; • **Information systems** → *Graph Anomaly Detection*.

ACM Reference Format:

Xiang Li, Jianpeng Qi, Zhongying Zhao, Guanjie Zheng, Lei Cao, Junyu Dong, and Yanwei Yu[†]. 2018. UMGAD: Unsupervised Multiplex Graph Anomaly Detection. In *Proceedings of Make sure to enter the correct conference title from your rights confirmation email (Conference acronym 'XX)*. ACM, New York, NY, USA, 15 pages. <https://doi.org/XXXXXXXX.XXXXXXX>

1 Introduction

Anomaly detection [7, 30], aimed at identifying entities that deviate significantly from normal conditions, is extensively utilized across various applications, for example, fraudulent user detection in financial networks [5, 9, 16, 24, 26], anomalous behavior detection in social networks [6, 31, 45], malicious comments in review networks [37], review-scrubbing buffs in e-commerce networks [48], and so on. Unlike time series anomaly detection, GAD presents greater challenges due to the inherent complexity of graph data [14, 44], which typically encompasses node attributes and structural features [38]. This complexity renders the task of capturing anomalies within graphs particularly formidable.

Due to the high cost of acquiring real anomaly data, a large number of existing GAD methods are performed in an unsupervised manner [40, 42, 43, 46], to detect instances that deviate significantly from the majority of the data. Various methods have been proposed to solve the unsupervised graph anomaly detection (UGAD) problem. They can be broadly categorized into the following types, *i.e.*, traditional methods, message passing-improved (MPI) methods, contrastive learning (CL)-based methods, and graph

[†]Corresponding author: Yanwei Yu (yuyanwei@ouc.edu.cn).

Permission to make digital or hard copies of all or part of this work for personal or classroom use is granted without fee provided that copies are not made or distributed for profit or commercial advantage and that copies bear this notice and the full citation on the first page. Copyrights for components of this work owned by others than the author(s) must be honored. Abstracting with credit is permitted. To copy otherwise, or republish, to post on servers or to redistribute to lists, requires prior specific permission and/or a fee. Request permissions from permissions@acm.org.

Conference acronym 'XX, June 03–05, 2018, Woodstock, NY

© 2018 Copyright held by the owner/author(s). Publication rights licensed to ACM.

ACM ISBN 978-1-4503-XXXX-X/18/06

<https://doi.org/XXXXXXXX.XXXXXXX>

autoencoder (GAE)-based methods. Early traditional UGAD methods [22] are usually based on machine learning algorithms to encode graph information and detect anomalies, or utilize residual information to capture anomalous features. Message passing-improved methods [29, 34] learn anomalous node features by improving the message-passing mechanism of GNNs. Recently, with the rapid development of graph neural networks (GNNs), more and more CL-based and GAE-based methods have emerged. For example, GRA-DATE [10] performs anomaly detection through a multi-scale contrastive learning network with augmented views, and VGod [17] combines variance-based and graph reconstruction-based models through contrastive learning to detect anomalies. ADA-GAD [15] builds a denoised graph first to train the graph encoder and then trains the graph decoder on the original graph for reconstructing node attributes and structure.

Challenges. Existing UGAD approaches, CL-based and GAE-based methods, have achieved promising results. Nevertheless, the UGAD task still faces the following two major challenges: (1) *Most existing methods focus solely on single-layer heterogeneous graphs, while real-world graphs are often multiplex.* Real-world graph data typically includes multiple types of interactions, such as clicking, adding, and buying between users and items in e-commerce networks, or different comments and rating scores in review networks. These interactions result in complex structures, known as multiplex heterogeneous graphs, which have increasingly attracted researchers' attention. Due to the complexity and diversity of interactions within these networks, the GAD task becomes more challenging, complicating the design of effective anomaly detection algorithms. (2) *In real unsupervised scenarios, most of the existing aspects face difficulties in selecting anomaly score thresholds because the number of anomalies is unknown.* Existing models typically employ two approaches to set the anomaly score threshold: first, by selecting the threshold based on the known number of anomalies when ground truth data is available; second, by choosing the threshold that yields the best model performance. However, these methods are not suitable when the number of anomalies and their labels are unknown, making it unreasonable to rely on these approaches for threshold selection in the unsupervised scenario.

Presented Work. Recognizing the above challenges, we focus on exploring the important impact of different interactive relations on node representation learning and extracting anomaly information through graph reconstructions for multiplex heterogeneous graphs, while finding appropriate anomaly score thresholds in the real unsupervised scenario to improve the anomaly detection performance of the model. To this end, this paper proposes a novel unsupervised multiplex graph anomaly detection method, named UMGAD. We first learn multi-relational correlations among nodes in multiplex heterogeneous graphs and capture anomaly information during node attribute and structure reconstruction through GMAE. Then, to further weaken the influence of noise and redundant information on abnormal information extraction, we generate attribute-level and subgraph-level augmented-view graphs respectively, and perform attribute and structure reconstruction through GMAE. Finally, We learn to optimize node attributes and structural features through contrastive learning between original-view and augmented-view graphs to improve the model's ability to capture

anomalies. Meanwhile, we also propose a new anomaly score threshold selection strategy, which allows the model to be independent of the ground truth in real unsupervised scenarios.

This work makes the following contributions:

- We propose a novel unsupervised multiplex graph anomaly detection method that emphasizes the importance of constructing and exploiting different interactions between nodes and addresses the problem of unsupervised anomaly detection in multiplex heterogeneous graphs.
- We design an effective method for selecting appropriate anomaly score thresholds in the real unsupervised scenario without involving the ground truth by performing anomaly information extraction on both the original- and the augmented-view graphs.
- We conduct extensive experiments on two datasets with injected anomalies and two with real anomalies to demonstrate the superiority of our proposed method. Experiment results show that UMGAD achieves 13.48%, and 11.68% average improvement in terms of AUC and macro-F1 across four datasets compared to SOTA baselines.

2 Related Work

UGAD has attracted increasing attention in recent years, many researchers focus on how to use self-supervised signals to improve the model's ability to detect anomalies in unsupervised scenarios. Early traditional UGAD methods, such as Radar [22] and ResGCN [33], which capture anomalous features by describing the residuals of attribute information and their consistency with network information, are concise and effective. With the rapid development of GNNs, it has also been naturally introduced into the field of anomaly detection, and recent researchers have been trying to develop UGAD models based on GNNs. We broadly categorize GNN-based models into three types: MPI methods, CL-based methods, and GAE-based methods.

MPI methods. It is well known that most of the GNN-based methods exploit the message passing mechanism [39] of GNN to learn node attributes by aggregating the neighborhood information of nodes. However, due to the feature inconsistency between normal and anomalous nodes, the original message passing mechanism may impair the model's ability to extract the anomalous information. Luo et al. [29] improve the message passing mechanism from the perspectives of community segmentation and community structure learning and obtain node attributes by introducing the community structure. Qiao et al. [34] propose a truncated affinity maximization method named TAM, which maximizes the local affinity of a node with its neighbor nodes and performs node characterization on the truncated graph instead of the original graph. by maximizing the local affinity between nodes and neighboring nodes, and performing node attribute learning on a truncated graph instead of the original graph.

CL-based methods. As a common method for mining self-supervised signals [20, 25, 27], contrastive learning is also introduced to the UGAD task [41] to capture feature inconsistencies between normal and anomalous nodes. CoLa [28] is a novel contrastive instance pair sampling method that leverages local information in network data to learn information embedding from high-dimensional attributes and local structures. Zhang et al. [47]

propose a self-supervised learning framework called Sub-CR that jointly optimizes two modules, multi-view contrastive-based learning, and attribute-based reconstruction, to more accurately detect anomalies on attribute networks. In addition to focusing on node attribute learning and attribute reconstruction, contrastive learning can also be extended to the subgraph level to capture complex structural anomalies. GRADATE [10], a multi-view and multi-scale contrastive learning framework including node-subgraph contrastive learning and subgraph-subgraph contrastive learning, can better capture different features between normal and abnormal substructures, which helps to identify complex structural anomalies. Huang et al. [17] combine variance-based models and attribute reconstruction models to detect outliers in a balanced way.

GAE-based methods: GAE-based methods [23] are one of the mainstay methods to detect anomalies by reconstructing the node attributes and structural features in the graphs. Ding et al. [8] use GCN to model graph topology and node attributes to learn node embeddings. Roy et al. [36] incorporate neighborhood reconstruction in their proposed GAD-NR, aiming to reconstruct the entire neighborhood of a node based on the corresponding node representation (including local structure, self-properties, and neighborhood properties). ADA-GAD [15] introduces a two-stage anomaly denoising autoencoder framework, where the first stage trains the GAE on the generated denoised graphs, and the second stage retains only the encoder and retrains the encoder on the original graphs while introducing regularization of the distribution of node anomalies to prevent anomalous overfitting.

3 Preliminary

Generally, a network is denoted as $\mathcal{G} = \{\mathcal{V}, \mathcal{E}, \mathcal{X}\}$, where \mathcal{V} is the collection of nodes, and \mathcal{E} is the collection of edges between the nodes, and \mathcal{X} is the collection of node attributes.

DEFINITION 1 (MULTIPLEX HETEROGENEOUS GRAPH). *Given the defined network \mathcal{G} , a multiplex heterogeneous graph can be divided into R relational subgraphs $\mathcal{G} = \{\mathcal{G}^1, \mathcal{G}^2, \dots, \mathcal{G}^R\}$, where R denotes the number of interactive relation categories. Each subgraph is defined as $\mathcal{G}^r = \{\mathcal{V}, \mathcal{E}^r, \mathcal{X}\}$, where \mathcal{V} and $\mathcal{X} \in \mathbb{R}^{|\mathcal{V}| \times f}$ denote the set of all nodes and node attributes respectively, f is the size of the node attribute, \mathcal{E}^r represents the edge set in the r -th relational subgraph, $\mathcal{R} = \{1, 2, \dots, R\}$ represents the set of edge relation categories, $|\mathcal{R}| = R$, and $\mathcal{E} = \bigcup_{r \in \mathcal{R}} \mathcal{E}^r$ is the collection edge set of various relation subgraphs.*

Next, we formally defined our studied problem in this work.

PROBLEM (UNSUPERVISED MULTIPLEX GRAPH ANOMALY DETECTION). *Given a multiplex graph \mathcal{G} , the unsupervised GAD problem aims to identify nodes that significantly deviate from the majority in both structural features and node attributes. We try to define an anomaly function $S(i)$ that assigns an anomaly score to each node $v_i \in \mathcal{V}$. Nodes with scores exceeding the selected anomaly threshold are classified as anomalous, while others are considered normal.*

4 Methodology

In this section, we propose a novel unsupervised multiplex graph anomaly detection method named UMGAD depicted in Fig. 1, which mainly includes three key components: (1) *Original-view Graph*

Reconstruction, (2) *Augmented-view Graph Reconstruction* and (3) *Dual-view Contrastive Learning*, to capture the anomalous information on both original and augmented graphs, and fuse the attribute and structural information of the nodes learned from the two views by contrastive learning to improve the model anomaly detection performance.

4.1 Original-view Graph Reconstruction

4.1.1 Attribute Reconstruction. Attribute inconsistency is one of the most important evidence to distinguish abnormal and normal nodes in the feature space. However, the aggregation mechanism of existing GNN models is based on the homogeneity assumption, which is detrimental to identifying rare abnormal nodes because most of the connected normal nodes will weaken the abnormal information during message propagation, thus smoothing the attribute inconsistency to hinder the abnormality detection. To fully utilize the inconsistency property in the feature space, we mask each relational subgraph with an attribute masking strategy. Formally, we get the subgraph \mathcal{G}^r and randomly sample a subset \mathcal{V}_{ma} with a masking ratio r_m and then obtain the perturbation subgraph as follows:

$$\mathcal{G}_{ma}^r = (\mathcal{V}, \mathcal{E}, \mathcal{X}_{ma}), \quad (1)$$

where the original node attributes in \mathcal{X}_{ma} are replaced by the [MASK] tokens which are learnable vectors. Masked nodes are selected by utilizing uniform random sampling without replacement, which helps prevent potential bias. $\mathcal{V}_{re} = \mathcal{V} - \mathcal{V}_{ma}$ denotes the set of remaining nodes that are unaffected by masking. We repeat the attribute masking strategy on each relational subgraph for K times to finally generate a set of masked subgraphs $\mathcal{G}_{ma}^r = \{\mathcal{G}_{ma}^{r,1}, \mathcal{G}_{ma}^{r,2}, \dots, \mathcal{G}_{ma}^{r,K}\}$ for \mathcal{G}^r . These masked subgraphs are then fed into the GNN-based encoder and decoder and the output of each encoder is as follows:

$$\mathcal{X}_{ma}^{r,k} = Dec(Enc(\mathcal{V}_{re}, \mathcal{E}^r | \mathbf{W}_{enc1}^{r,k}), \mathcal{E}^r | \mathbf{W}_{dec1}^{r,k}), \quad (2)$$

where $\mathcal{X}_{ma}^{r,k} \in \mathbb{R}^{|\mathcal{V}| \times f}$ is the output of the attribute decoder in the k -th masking repeat of the r -th relational subgraph, $\mathbf{W}_{enc1}^{r,k} \in \mathbb{R}^{f \times d_h}$ and $\mathbf{W}_{dec1}^{r,k} \in \mathbb{R}^{d_h \times f}$ are the trainable weight matrices. Inside each encoder and decoder, before the vertical lines | are the input variables after the vertical lines are the important learnable weights. In subsequent formulas, the vertical line | means the same thing.

Considering the multi-relational correlations among nodes and the importance of different relational subgraphs, we aggregate all subgraphs by using a set of learnable weight parameters as follows:

$$\tilde{\mathcal{X}}_{ma}^k = \sum_{r=1}^R a^r \mathcal{X}_{ma}^{r,k}. \quad (3)$$

Finally, to optimize the attribute reconstruction process, we compute the reconstruction error between the aggregated node attributes and the original attributes of the masked nodes as follows:

$$\mathcal{L}_A = \sum_{k=1}^K \frac{1}{|\mathcal{V}_{ma}^k|} \sum_{v_i \in \mathcal{V}_{ma}^k} \left(1 - \frac{\tilde{x}_{ma}^k(i)^\top x(i)}{\|\tilde{x}_{ma}^k(i)\| \cdot \|x(i)\|}\right)^\eta, \eta \geq 1, \quad (4)$$

which is the average of all masked nodes, where \mathcal{V}_{ma}^k is the k -th masked node subset, $\tilde{x}_{ma}^k(i)$ denotes the i -th reconstructed node attribute vector in $\mathcal{X}_{ma}^{r,k}$, $x(i)$ denotes the i -th original node attribute

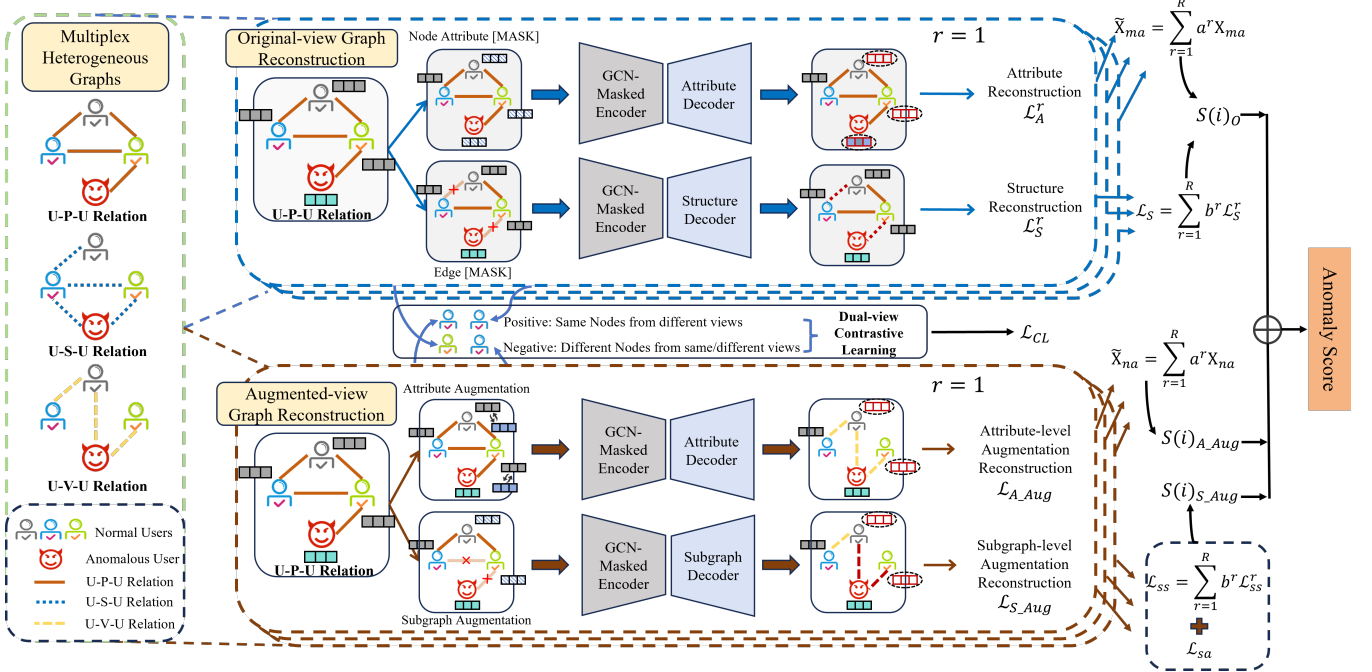


Figure 1: The overview of the proposed UMGAD. There are three interaction types in the multiplex heterogeneous graph: U-P-U links users reviewing at least one product, U-S-U link users having at least one identical star rating within a week, U-V-U links linguistically similar users.

vector in \mathcal{X} . The scaling factor η is a hyperparameter that can be adjusted on different datasets.

4.1.2 Structure Reconstruction. In addition to attribute anomalies, structural anomalies are also more difficult to recognize, they can be camouflaged by mimicking the attributes of normal nodes. However, structural inconsistencies are reflected in the connections, and if the target node is not well reconstructed structurally, then it is likely to be anomalous.

We capitalize on the inconsistency of the structure space and propose to perturb the subgraph through a structural masking strategy that works to break short-range connections, causing nodes to look elsewhere for evidence that suits them. Similarly, we use masking ratios r_m to randomly sample a subset of edges from the edges observed in the subgraph and then obtain the corresponding perturbed subgraph as follows:

$$\mathcal{G}_{ms}^r = (\mathcal{V}, \mathcal{E}^r \setminus \mathcal{E}_{ms}^r, \mathcal{X}), \quad (5)$$

where $\mathcal{E}^r \setminus \mathcal{E}_{ms}^r = \mathcal{E}^r - \mathcal{E}_{ms}^r$ denotes the remaining edges set after edge masking in the r -th subgraph. We utilize the same random sampling method to select the masked edges. Similarly, we repeat the structure masking strategy on all relational subgraphs for K times to finally generate a set of masked subgraphs $\mathcal{G}_{ms}^r = \{\mathcal{G}_{ms}^{r,1}, \mathcal{G}_{ms}^{r,2}, \dots, \mathcal{G}_{ms}^{r,K}\}$ for each relational subgraph \mathcal{G}^r , which are further fed into the GNN-based encoder and decoder to learn the node attribute:

$$\mathcal{X}_{ms}^{r,k} = \text{Dec}(\text{Enc}(\mathcal{V}, \mathcal{E}^r \setminus \mathcal{E}_{ms}^{r,k} | \mathbf{W}_{enc2}^{r,k}), \mathcal{E}^r \setminus \mathcal{E}_{ms}^{r,k} | \mathbf{W}_{dec2}^{r,k}), \quad (6)$$

where $\mathcal{X}_{ms}^{r,k} \in \mathbb{R}^{|\mathcal{V}| \times f}$ is the output of the attribute decoder in the k -th masking repeat of the r -th relational subgraph, $\mathbf{W}_{enc2}^{r,k} \in \mathbb{R}^{f \times d_h}$ and $\mathbf{W}_{dec2}^{r,k} \in \mathbb{R}^{d_h \times f}$ are the trainable weight matrices. In contrast

to the reconstruction goal of masking attributes, we use the edge set of the k -th masked sampling subgraph of the r -th relational subgraph, $\mathcal{E}_{ms}^{r,k}$, as a self-supervised signal to recover the original subgraph structure by predicting the masked edges with the cross-entropy function as follows:

$$\mathcal{L}_S^r = \sum_{k=1}^K \sum_{(v,u) \in \mathcal{E}_{ms}^{r,k}} \log \frac{\exp(g(v,u))}{\sum_{(v,u') \in \mathcal{E}_{ms}^{r,k}} \exp(g(v,u'))}, \quad (7)$$

where $g(v,u) = \mathbf{x}_{ms}^{r,k}(v)^\top \mathbf{x}_{ms}^{r,k}(u)$ denotes the estimated probability of the link between node v and u . Note that we introduce negative sampling to train a more generalized model by accumulating all edge prediction probabilities of the unmasked subgraphs in the denominator, making the model robust to external noise. Considering the importance of different relational subgraphs for structure reconstruction, we aggregate all subgraph structure reconstruction losses together using a set of learnable weight parameters as follows:

$$\mathcal{L}_S = \sum_{r=1}^R b^r \mathcal{L}_S^r. \quad (8)$$

The learned embedding captures anomalies in the attribute and structure space by jointly masking the attributes and edge reconstruction of the subgraph. Finally, the training objective for the original-view graph reconstruction is defined as follows:

$$\mathcal{L}_O = \alpha \mathcal{L}_A + (1 - \alpha) \mathcal{L}_S. \quad (9)$$

4.2 Augmented-view Graph Reconstruction

Due to the small number of anomalies in the graph, graphs containing anomalous nodes are usually unbalanced, which leads to a lot of noise or redundant information in the graph. Therefore,

we introduce three simplified graph masking strategies to generate two levels of augmented graphs, namely: attribute-level augmented graph and subgraph-level augmented graph, to reduce the redundant information in the original graph.

4.2.1 Attribute-level Augmented Graph Reconstruction. For attribute-level augmented graph reconstruction, we randomly select a subset of nodes $\mathcal{V}_{na} \subset \mathcal{V}$ for replacement-based augmentation. The selected node features are adjusted as follows:

$$\tilde{x}_i = \begin{cases} x_j, & v_i \in \mathcal{V}_{na} \\ x_i, & v_i \in \mathcal{V} \setminus \mathcal{V}_{na} \end{cases}, \quad (10)$$

where $\mathcal{V} \setminus \mathcal{V}_{na} = \mathcal{V} - \mathcal{V}_{na}$. We randomly select another node v_j and replace the original feature x_i of v_i with the feature x_j of node v_j if $v_i \in \mathcal{V}_{na}$. We also introduce the masking mechanism where the feature of each node $v_i \in \mathcal{V}_{na}$ is masked.

We repeat the above augmentation operation for K times to generate a collection of the attribute-level augmented graphs for each relational subgraph \mathcal{G}^r , denoted as $\mathcal{G}_{na}^r = \{\mathcal{G}_{na}^{r,1}, \mathcal{G}_{na}^{r,2}, \dots, \mathcal{G}_{na}^{r,K}\}$, where each $\mathcal{G}_{na}^{r,k} = (\mathcal{V}, \mathcal{E}^r, \tilde{\chi}_{na}^{r,k})$, and $\tilde{\chi}_{na}^{r,k}$ is the augmented attribute matrix generated each time. We feed each $\mathcal{G}_{na}^{r,k}$ into the attribute-level GMAE consisting of the simplified GCN encoder and decoder with masking mechanism, and then we can obtain the reconstructed node embedding matrix $\chi_{na}^{r,k}$ as follows:

$$\chi_{na}^{r,k} = Dec(Enc(\mathcal{V}, \mathcal{E}^r | \mathbf{W}_{enc3}^{r,k}), \mathcal{E}^r | \mathbf{W}_{enc3}^{r,k}). \quad (11)$$

Similarly, we aggregate all subgraph attributes together using a set of learnable weight parameters as follows:

$$\tilde{\chi}_{na}^k = \sum_{r=1}^R a^r \chi_{na}^{r,k}. \quad (12)$$

Then, the training objective for the attribute-level augmented-view graph reconstruction is defined as follows:

$$\mathcal{L}_{A_Aug} = \sum_{k=1}^K \frac{1}{|\mathcal{V}_{na}^k|} \sum_{v_i \in \mathcal{V}_{na}^k} \left(1 - \frac{\tilde{\chi}_{na}^k(i)^\top x(i)}{\|\tilde{\chi}_{na}^k(i)\| \cdot \|x(i)\|}\right)^\eta, \eta \geq 1, \quad (13)$$

where $|\mathcal{V}_{na}^k|$ is the k -th masked subset, $\tilde{\chi}_{na}^k(i)$ denotes the reconstructed node attribute vector in $\chi_{na}^{r,k}$, $x(i)$ denotes the original node attribute vector in \mathcal{X} .

4.2.2 Subgraph-level Augmented Graph Reconstruction. We propose a subgraph masking mechanism that employs a subgraph sampling strategy based on random walk with restart (RWR) for subgraph sampling and masks these sampled subgraphs for each relational subgraph \mathcal{G}^r in the multiplex heterogeneous graph \mathcal{G} , then we obtain the subgraph-level augmented graphs collection $\mathcal{G}_s^r = \{\mathcal{G}_s^{r,1}, \mathcal{G}_s^{r,2}, \dots, \mathcal{G}_s^{r,K}\}$, where each $\mathcal{G}_s^{r,k} = (\mathcal{V}, \mathcal{E}^r \setminus \mathcal{E}_s^r, \chi_s^{r,k}, \mathcal{E}_s^r$ and $\chi_s^{r,k})$ are the edge subset and attribute matrix generated each time.

Subgraph level augmentation can be considered as a specific combination of node attribute level and structure level augmentation. The reconstructed node attribute matrix $\tilde{\chi}_s^k$ and structural adjacent matrix $\tilde{\mathbf{A}}_s^r$ are shown below, respectively:

$$\tilde{\chi}_s^k = \sum_{r=1}^R a^r \chi_s^{r,k}, \tilde{\mathbf{A}}_s^r = \sum_{r=1}^R \sigma(\tilde{\chi}_s^r \tilde{\chi}_s^r). \quad (14)$$

Then the subgraph-level augmented attribute and structure reconstruction loss values \mathcal{L}_{sa} and \mathcal{L}_{ss} is defined as follows:

$$\mathcal{L}_{sa} = \frac{1}{|\mathcal{V}_s^k|} \sum_{k=1}^l \sum_{v_i \in \mathcal{V}_s^k} \left(1 - \frac{\tilde{\chi}_s^k(i)^\top x(i)}{\|\tilde{\chi}_s^k(i)\| \cdot \|x(i)\|}\right)^\eta, \eta \geq 1, \\ \mathcal{L}_{ss} = \sum_{r=1}^R b^r \sum_{k=1}^l \sum_{(v,u) \in \mathcal{E}_s^{r,k}} \log \frac{\exp(g(v,u))}{\sum_{(v,u') \in \mathcal{E}_s^{r,k}} \exp(g(v,u'))}, \quad (15)$$

where $\tilde{\chi}_s^k(i)$ and $x(i)$ are the attribute-level augmented embedding and original node attribute respectively, and $g(v,u) = x_s^{r,k}(v)^\top x_s^{r,k}(u)$ denotes the estimated probability of the link between node v and u .

Finally, the training objective for the subgraph-level augmented-view graph reconstruction is defined as follows:

$$\mathcal{L}_{S_Aug} = \beta \mathcal{L}_{sa} + (1 - \beta) \mathcal{L}_{ss}. \quad (16)$$

4.3 Dual-view Contrastive Learning

Dual-view contrastive learning is defined between two views, the original view, and the augmented view, to learn more representative and intrinsic node embeddings for GAD tasks, which will help capture anomaly information. Specifically, we optimize the node attribute under joint loss by comparing the original-view graph with the attribute-level augmented-view graph and the subgraph-level augmented-view graph, respectively. The node v_i 's attribute in the original view forms a positive pair with the augmented view and a negative pair with another node v_j 's attribute in the original and augmented views. We use the following loss function to optimize contrastive learning:

$$\mathcal{L}_{cl}^{oa} = - \sum_{i=1}^{|\mathcal{V}|} \log \frac{\exp(\tilde{x}_{ma}(i) \cdot \tilde{x}_{na}(i))}{\exp(\tilde{x}_{ma}(i) \cdot \tilde{x}_{ma}(j)) + \exp(\tilde{x}_{ma}(i) \cdot \tilde{x}_{na}(j))}, \\ \mathcal{L}_{cl}^{os} = - \sum_{i=1}^{|\mathcal{V}|} \log \frac{\exp(\tilde{x}_{ma}(i) \cdot \tilde{x}_s(i))}{\exp(\tilde{x}_{ma}(i) \cdot \tilde{x}_{ma}(j)) + \exp(\tilde{x}_{ma}(i) \cdot \tilde{x}_s(j))}, \quad (17)$$

where \mathcal{L}_{cl}^{oa} represents the contrastive loss between the original-view graph and the attribute-level augmented-view graph, \mathcal{L}_{cl}^{os} represents the contrastive loss between the original-view graph and the subgraph-level augmented-view graph.

The final loss dual-view contrastive learning is $\mathcal{L}_{CL} = \mathcal{L}_{cl}^{oa} + \mathcal{L}_{cl}^{os}$.

4.4 Optimization Objective

Putting it all together, we have the overall loss function in the training stage is as follows:

$$\mathcal{L} = \mathcal{L}_O + \lambda \mathcal{L}_{A_Aug} + \mu \mathcal{L}_{S_Aug} + \Theta \mathcal{L}_{CL}, \quad (18)$$

where λ , μ , and Θ are hyperparameters that measure the importance of different augmented views and contrastive learning.

Based on the final training loss \mathcal{L} , we train several autoencoder modules, sort the nodes based on their anomaly scores, $S(i)$, and treat the nodes with higher $S(i)$ as anomalous nodes. For both original-view and augmented-view graphs, we use the following formula to calculate and finally take the arithmetic average of

Table 1: Statistical information of evaluation datasets. #Ano. denotes the number of anomalies, (I) represents the injected anomalies, and (R) represents the real anomalies.

Datasets	#Nodes	#Ano. (I/R)	Relation Type	#Edges
Retail	32,287	300 (I)	View	75,374
			Cart	12,456
			Buy	9,551
Alibaba	22,649	300 (I)	View	34,933
			Cart	6,230
			Buy	4,571
Amazon	11,944	821 (R)	U-P-U	175,608
			U-S-U	3,566,479
			U-V-U	1,036,737
YelpChi	45,954	6674 (R)	R-U-R	49,315
			R-S-R	3,402,743
			R-T-R	573,616

multiple views as the anomaly score of the node v_i :

$$S(i)_{O/A_Aug/S_Aug} = \varepsilon \cdot \frac{1}{R} \sum_{r=1}^R \|\tilde{a}(i)^r_{O/A_Aug/S_Aug} - a(i)^r\|_1 + (1 - \varepsilon) \cdot \|\tilde{x}_{O/A_Aug/S_Aug}(i) - x(i)\|_2, \quad (19)$$

where $S(i)_{O/A_Aug/S_Aug}$ denotes the score in specific graph, $\|\cdot\|_1$ denotes the L1-norm of the vector, $\|\cdot\|_2$ denotes the Euclidean norm of a vector, $\tilde{a}(i)^r$ and $a(i)^r$ represent the i -th row of the specific reconstructed structure matrix $\tilde{A}^r_{O/A_Aug/S_Aug}$ and original structure matrix A^r , respectively. Similarly, $\tilde{x}(i)$ and $x(i)$ are the reconstructed attribute vector and the original attribute vector of the node v_i , respectively.

5 Experiments

In this section, we evaluate the performance of our proposed method through extensive experiments and answer the following questions:

- **(RQ1)** How does UMGAD effectively alleviate the difficulty of selecting anomaly score thresholds in unsupervised GAD?
- **(RQ2)** How does UMGAD perform compared to other GAD methods in a real unsupervised scenario?
- **(RQ3)** What are the effects of different modules in UMGAD on performance?
- **(RQ4)** How do different hyperparameter settings affect the performance?
- **(RQ5)** How does UMGAD perform compared to other GAD methods in the scenario of threshold selection with ground truth leakage? *The experimental results can be found in the Supplement.*

5.1 Experimental Settings

5.1.1 Dataset. We have conducted experiments on two datasets injected with synthetic anomalies: Retail_Rocket [35] (Retail for short) and Alibaba [13], and two real-world publicly available datasets with anomalies: Amazon [9] and YelpChi [21]. *The detailed description of these datasets is shown in the supplementary material.*

5.1.2 Baselines. We compare with four categories of methods on the unsupervised GAD task.

- **Traditional methods:** Radar [22].

- **MPI methods:** ComGA [29] and TAM [34].
- **CL-based methods:** CoLA [28], ANEMONE [18], Sub-CR [47], ARISE [11], SL-GAD [49], PREM [32], GCCAD [2], GRADATE [10], and VGOD [17].
- **GAE-based methods:** GCNAE [19], DOMINANT [8], Anomaly-DAE [12], AdONE [1], GAD-NR [36], ADA-GAD [15], GADAM [3] and AnomMAN [4].

5.1.3 Implementation Details. We implement all baseline methods according to their provided code or utilizing the PyGOD toolkit. We set the epoch number, dropout rate, and weight decay to 100, 0.1, and 0.01, respectively, and the embedding dimension d to 32, and our method uses Simplified GCN as the encoder and decoder. For Amazon and YelpChi datasets with real anomalies, the number of encoder layers is set to 2 and the depth of the decoder is set to 1. For the artificial datasets with injected anomalies, the number of encoder and decoder layers are both set to 1. During the augmentation period, the number of node masks and edges is set to 1 to 20. The number of SL-GAD on excursions and the excursion length of the subgraph masks are set to 2, and K are set to 10. The pre-training epoch and the retention epoch are both set to 20. AUC (area under the ROC curve) and Macro-F1 are used as performance metrics.

5.2 Anomaly Score Threshold Selection for Unsupervised Anomaly Detection (RQ1)

For the unsupervised graph anomaly detection task, since the nodes' label (normal or abnormal) is unknown, a common approach is to compute the anomaly score for each node and rank them in order of the anomaly score from high to low. Nodes with high anomaly scores are considered anomalous nodes. However, determining a more accurate anomaly score threshold has always been a difficult problem in unsupervised graph anomaly detection. A good unsupervised anomaly detection model with its calculated anomaly scores for normal and abnormal nodes should be easy to distinguish, and the thresholds for dividing the abnormal nodes from the normal nodes are also relatively easy to set. To find a suitable anomaly score threshold, we visualize the ranked node anomaly scores of different methods and the corresponding threshold selection strategy, *i.e.*, we select the anomaly score value of the convergence *tangent point* in the anomaly score curve as the anomaly score threshold. The results on two datasets with real anomalies are shown in Fig. 2, and the results on two datasets with injected anomalies are shown in Fig. 5 in the Supplement.

In Fig. 2, we show the trend of the ranked node anomaly scores for the best-performing baselines, TAM, ADA-GAD, GADAM, and AnomMAN, as well as for our UMGAD, on Amazon and YelpChi respectively. As can be seen in Fig. 2, compared with the other four best-performing baselines, the curve of our UMGAD can converge quickly (become stable) to a position closer to the actual number of anomalies in the datasets. It allows UMGAD to better distinguish the anomaly scores of anomalous nodes from those of normal nodes, and thus be able to identify anomalies more accurately. A good unsupervised anomaly detection model should be able to clearly distinguish the anomaly scores of abnormal nodes from those of normal nodes. Therefore, we use the anomaly score at the convergence of the curve as the anomaly score threshold. After

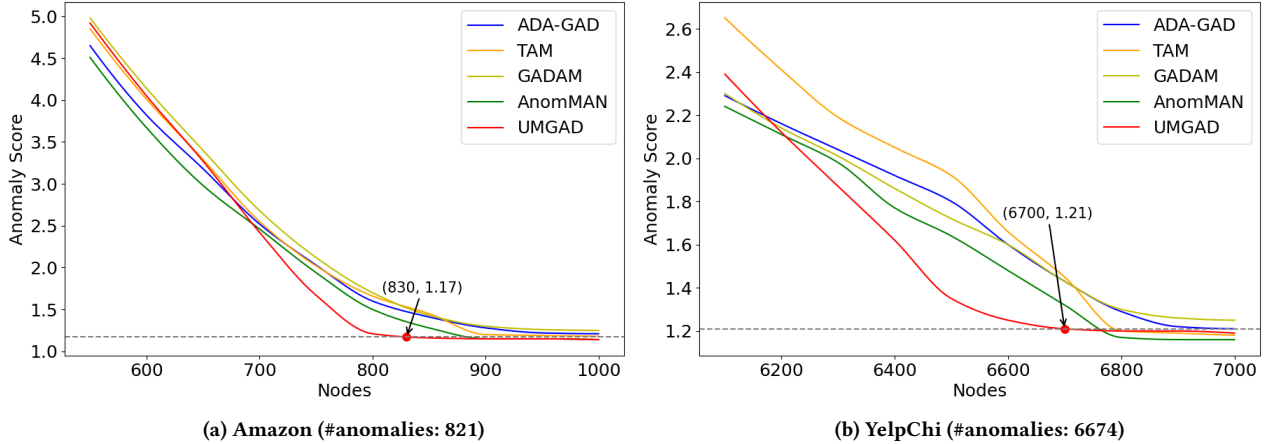


Figure 2: Visualization of ranked node anomaly scores for SOTA methods on two datasets with real anomalies.

Table 2: Performance comparison of all models on four datasets in the real unsupervised scenario. Marker * indicates the results are statistically significant (t-test with p-value < 0.01).

Method		Retail		Alibaba		Amazon		YelpChi	
		AUC	Macro-F1	AUC	Macro-F1	AUC	Macro-F1	AUC	Macro-F1
Traditional	Radar	0.625	0.533	0.659	0.560	0.582	0.525	0.502	0.485
MPI	ComGA	0.665	0.623	0.692	0.603	0.661	0.691	0.514	0.491
	TAM	0.688	0.650	0.712	0.660	<u>0.763</u>	0.637	0.546	<u>0.538</u>
CL-based	CoLA	0.554	0.513	0.570	0.541	0.582	0.522	0.444	0.468
	ANEMONE	0.630	0.589	0.651	0.581	0.622	0.550	0.503	0.492
	Sub-CR	0.650	0.594	0.652	0.599	0.599	0.530	0.489	0.490
	ARISE	0.671	0.635	0.708	0.619	0.692	0.612	0.532	0.503
	SL-GAD	0.658	0.596	0.700	0.611	0.653	0.585	0.522	0.484
	PREM	0.661	0.609	0.680	0.607	0.658	0.588	0.521	0.493
	GCCAD	0.665	0.611	0.701	0.630	0.662	0.591	0.522	0.497
	GRADATE	0.683	0.644	0.702	0.642	0.730	0.661	0.540	0.521
	VGOD	0.680	0.639	0.710	0.644	0.724	0.702	0.538	0.510
GAE-based	DOMINANT	0.621	0.577	0.609	0.549	0.621	0.581	0.500	0.490
	GCNAE	0.623	0.579	0.624	0.564	0.607	0.583	0.502	0.494
	AnomalyDAE	0.618	0.525	0.665	0.571	0.634	0.588	0.523	0.496
	AdONE	0.621	0.565	0.641	0.579	0.649	0.601	0.520	0.505
	GAD-NR	0.681	0.632	0.707	0.658	0.752	0.681	0.540	0.531
	ADA-GAD	0.688	<u>0.650</u>	<u>0.715</u>	<u>0.663</u>	0.754	0.687	<u>0.545</u>	0.530
	GADAM	<u>0.690</u>	0.644	0.712	0.656	0.756	0.687	0.545	0.535
	AnomMAN	0.688	0.645	0.710	0.650	0.758	<u>0.689</u>	0.542	0.536
	UMGAD	0.770*	0.722*	0.825*	0.740*	0.878*	0.779*	0.608*	0.597*
<i>Improvement</i>		11.92% ↑	11.08% ↑	15.38% ↑	11.61% ↑	15.07% ↑	13.06% ↑	11.56% ↑	10.97% ↑

introducing the ground truth we find that the number of anomalous nodes corresponding to the threshold selected by our UMGAD is very close to the real number of anomalies, which proves that our method can effectively alleviate the difficult problem of selecting anomaly score thresholds in the UGAD problem. *The experimental results in Retail and Alibaba dataset are shown in the Supplement.*

5.3 Performance Comparison in the Real Unsupervised Scenario (RQ2)

Next, we evaluate the performance of our UMGAD and all baselines in real unsupervised scenarios. That is, we use the convergence

point of the ranked anomaly score curve as the anomaly score threshold for each method. This threshold selection method does not require the introduction of any ground-truth information and is suitable for real unsupervised anomaly detection scenarios. The experimental results are shown in Table 2. The best results are highlighted in bold, and the second-best results are underlined.

As we can see, our UMGAD achieves the optimal performance, significantly outperforming all baselines in both AUC and macro-F1 metrics on four datasets, with specific emphasis on the improvement relative to the SOTA methods.

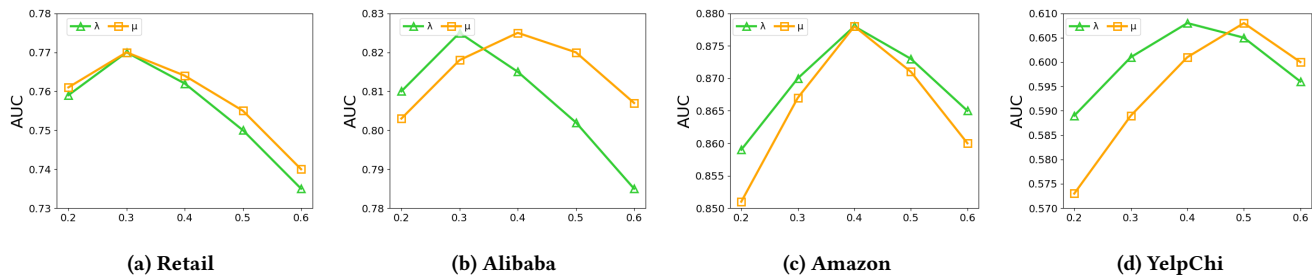
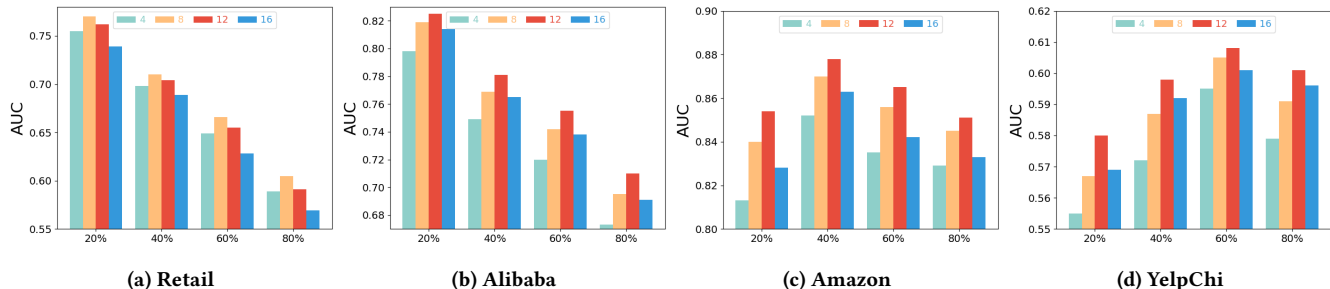
Figure 3: The effect of hyperparameters λ and μ in the final loss function.

Figure 4: The effect of masking ratio and masking subgraph size. The X-axis indicates the mask ratio, and 4 to 16 in the legend indicates the subgraph size.

We can draw the following conclusions: first, according to our proposed threshold selection strategy and the node anomaly score curves in Fig. 2, the number of detected anomalies corresponding to our selected thresholds is the closest to the real situation compared to other methods; second, our UMGAD method considers the multi-relational correlation between nodes, and mitigates the effects of noise and redundant information by introducing enhanced views that allow the model to capture the anomaly information more efficiently so that the anomaly scores of anomalous nodes can be better distinguished from those of normal nodes.

Table 3: The comparison of UMGAD and its variants on AUC and macro-F1 (F1 for short) metrics.

Dataset Metrics	Retail		Alibaba		Amazon		YelpChi	
	AUC	F1	AUC	F1	AUC	F1	AUC	F1
w/o M	0.712	0.669	0.783	0.689	0.829	0.716	0.571	0.556
w/o O	0.720	0.682	0.788	0.696	0.835	0.727	0.577	0.565
w/o NA	0.731	0.690	0.795	0.706	0.842	0.735	0.582	0.575
w/o SA	0.726	0.685	0.788	0.701	0.839	0.730	0.580	0.567
w/o DCL	0.748	0.702	0.806	0.718	0.848	0.755	0.588	0.577
UMGAD	0.770	0.722	0.825	0.740	0.878	0.779	0.608	0.597

5.4 Ablation Study (RQ3)

To evaluate the effectiveness of each component in UMGAD, we further conduct ablation studies on different variants. Specifically, we generate five variants as follows:

- **w/o M** removes GMAE and uses corresponding GAE instead.
- **w/o O** removes the original-view graph-masked autoencoder and only detects augmented graphs.
- **w/o NA** excludes the node attribute-level augmentation.
- **w/o SA** excludes the subgraph-level augmentation.

- **w/o DCL** excludes the dual-view contrastive learning.

Table 3 shows the results for variants on four datasets in real unsupervised scenarios. Our five variants perform worse than UMGAD in terms of AUC and macro-F1 metrics, which confirms the necessity and effectiveness of the proposed components. Among them, **w/o M** performs the worst, which demonstrates the effectiveness of graph-masked autoencoder for GAD tasks, because it is difficult to reconstruct the attribute and structural features of anomalous nodes well using only ordinary GAE, which leads to the insufficient ability of the model to detect anomalies. **w/o O** performs only better than **w/o M**, which demonstrates the importance of the original multiplex heterogeneous graph. Ignoring the original graph and only detecting anomalies in the augmented graph may result in the loss of some of the original anomaly information. Meanwhile, based on the experimental results of **w/o NA** and **w/o SA**, we can find that the augmented-view GMAE can capture anomalous information, which is difficult for original-view GMAE, because node attributes and structural features in the augmented graph have changed, mitigating the problem that GNN-based autoencoders are prone to fall into the homogeneity trap. **w/o CDL** performs the best of all variants, but is still worse than UMGAD, which demonstrates the importance of learning to optimize node attribute through dual-view contrastive learning.

5.5 Parameter Sensitivity Analysis (RQ4)

5.5.1 The effect of hyperparameters λ , and μ in the final loss function. λ and μ correspond to the importance parameters of the two enhanced views, respectively. Considering node attribute-level and subgraph-level enhanced views on top of the original view can improve the model performance, and the results of the parameter sensitivity experiments are shown in Fig. 3. The model performance is optimal when λ and μ are set to 0.3 and 0.3, 0.3 and 0.4, 0.4 and 0.4, and 0.4 and 0.5 on the four datasets, respectively.

5.5.2 *The effect of masking ratio r_m and masking subgraph size $|\mathcal{V}_m|$.* To investigate how these two main factors change the performance of our model, we analyze the trend of different values on four datasets. The values of subgraph size $|\mathcal{V}_m|$ (i.e., the number of nodes in the subgraph) are selected in $\{4, 8, 12, 16\}$, masking ratio r_m range in $\{20\%, 40\%, 60\%, 80\%\}$. From the results in Fig. 4, we can summarize that: (1) For YelpChi and Amazon, they achieve the best performance at 60% and 40% masking rate respectively. While Retail and Alibaba enjoy higher performance with 20% masking. The possible reason is that the anomaly rate of YelpChi and Amazon is higher than that of Retail and Alibaba, which allows YelpChi and Amazon to have relatively abundant self-supervised signals to reorganize the masked node information. (2) Removing some unnecessary connections helps to anomalously reduce the amount of redundant information propagated from the normal majority.

6 Conclusion

In this work, we propose a model called UMGAD for unsupervised multiplex graph anomaly detection tasks. Specifically, we reconstruct node attributes and structures and learn multi-relational correlations among nodes from two views: the original view and the augmented view. UMGAD mitigates the effects of redundant information and noise on attribute and structure reconstruction through the augmented view, and captures anomalous information through dual-view contrastive learning. Extensive experiments on two datasets with injected anomalies and two real-world datasets with real anomalies show that UMGAD outperforms SOTA methods in real unsupervised scenarios. Further ablation studies validate the effectiveness of each component of our model.

References

- [1] Sambaran Bandyopadhyay, Lokesh N, Saley Vishal Vivek, and M Narasimha Murty. 2020. Outlier resistant unsupervised deep architectures for attributed network embedding. In *Proceedings of the 13th international conference on web search and data mining*. 25–33.
- [2] Bo Chen, Jing Zhang, Xiaokang Zhang, Yuxiao Dong, Jian Song, Peng Zhang, Kaibo Xu, Evgeny Kharlamov, and Jie Tang. 2022. Gccad: Graph contrastive coding for anomaly detection. *IEEE Transactions on Knowledge and Data Engineering* 35, 8 (2022), 8037–8051.
- [3] Jingyan Chen, Guanghui Zhu, Chunfeng Yuan, and Yihua Huang. 2024. Boosting Graph Anomaly Detection with Adaptive Message Passing. In *The Twelfth International Conference on Learning Representations*.
- [4] Ling-Hao Chen, He Li, Wanyuan Zhang, Jianbin Huang, Xiaoke Ma, Jiangtao Cui, Ning Li, and Jaesoo Yoo. 2023. AnomMAN: Detect anomalies on multi-view attributed networks. *Information Sciences* 628 (2023), 1–21.
- [5] Tianyi Chen and Charalampos Tsourakakis. 2022. Antibenford subgraphs: Unsupervised anomaly detection in financial networks. In *Proceedings of the 28th ACM SIGKDD Conference on Knowledge Discovery and Data Mining*. 2762–2770.
- [6] Lu Cheng, Ruocheng Guo, Kai Shu, and Huan Liu. 2021. Causal understanding of fake news dissemination on social media. In *Proceedings of the 27th ACM SIGKDD Conference on Knowledge Discovery & Data Mining*. 148–157.
- [7] Kaize Ding, Jundong Li, Nitin Agarwal, and Huan Liu. 2021. Inductive anomaly detection on attributed networks. In *Proceedings of the twenty-ninth international conference on international joint conferences on artificial intelligence*. 1288–1294.
- [8] Kaize Ding, Jundong Li, Rohit Bhanushali, and Huan Liu. 2019. Deep anomaly detection on attributed networks. In *Proceedings of the 2019 SIAM international conference on data mining*. SIAM, 594–602.
- [9] Yingtong Dou, Zhiwei Liu, Li Sun, Yutong Deng, Hao Peng, and Philip S Yu. 2020. Enhancing graph neural network-based fraud detectors against camouflaged fraudsters. In *Proceedings of the 29th ACM international conference on information & knowledge management*. 315–324.
- [10] Jingcan Duan, Siwei Wang, Pei Zhang, En Zhu, Jingtao Hu, Hu Jin, Yue Liu, and Zhibin Dong. 2023. Graph anomaly detection via multi-scale contrastive learning networks with augmented view. In *Proceedings of the AAAI conference on artificial intelligence*, Vol. 37. 7459–7467.
- [11] Jingcan Duan, Bin Xiao, Siwei Wang, Haifang Zhou, and Xinwang Liu. 2023. Arise: Graph anomaly detection on attributed networks via substructure awareness. *IEEE transactions on neural networks and learning systems* (2023).
- [12] Haoyi Fan, Fengbin Zhang, and Zuoqiong Li. 2020. Anomalydae: Dual autoencoder for anomaly detection on attributed networks. In *ICASSP 2020-2020 IEEE International Conference on Acoustics, Speech and Signal Processing (ICASSP)*. IEEE, 5685–5689.
- [13] Chaofan Fu, Guanjie Zheng, Chao Huang, Yanwei Yu, and Junyu Dong. 2023. Multiplex heterogeneous graph neural network with behavior pattern modeling. In *Proceedings of the 29th ACM SIGKDD Conference on Knowledge Discovery and Data Mining*. 482–494.
- [14] Yuan Gao, Xiang Wang, Xiangnan He, Zhengguang Liu, Huamin Feng, and Yongdong Zhang. 2023. Addressing heterophily in graph anomaly detection: A perspective of graph spectrum. In *Proceedings of the ACM Web Conference 2023*. 1528–1538.
- [15] Junwei He, Qianqian Xu, Yangbanyan Jiang, Zitai Wang, and Qingming Huang. 2024. ADA-GAD: Anomaly-Denoised Autoencoders for Graph Anomaly Detection. In *Proceedings of the AAAI Conference on Artificial Intelligence*, Vol. 38. 8481–8489.
- [16] Xuanwen Huang, Yang Yang, Yang Wang, Chunping Wang, Zhisheng Zhang, Jiarong Xu, Lei Chen, and Michalis Vazirgiannis. 2022. Dgraph: A large-scale financial dataset for graph anomaly detection. *Advances in Neural Information Processing Systems* 35 (2022), 22765–22777.
- [17] Yihong Huang, Liping Wang, Fan Zhang, and Xuemin Lin. 2023. Unsupervised graph outlier detection: Problem revisit, new insight, and superior method. In *2023 IEEE 39th International Conference on Data Engineering (ICDE)*. IEEE, 2565–2578.
- [18] Ming Jin, Yixin Liu, Yu Zheng, Lianhua Chi, Yuan-Fang Li, and Shirui Pan. 2021. Anemone: Graph anomaly detection with multi-scale contrastive learning. In *Proceedings of the 30th ACM international conference on information & knowledge management*. 3122–3126.
- [19] Thomas N Kipf and Max Welling. 2016. Variational graph auto-encoders. *arXiv preprint arXiv:1611.07308* (2016).
- [20] Xiangjie Kong, Wenyi Zhang, Hui Wang, Mingliang Hou, Xin Chen, Xiaoran Yan, and Sajal K Das. 2024. Federated Graph Anomaly Detection via Contrastive Self-Supervised Learning. *IEEE Transactions on Neural Networks and Learning Systems* (2024).
- [21] Srijan Kumar, Xikun Zhang, and Jure Leskovec. 2019. Predicting dynamic embedding trajectory in temporal interaction networks. In *Proceedings of the 25th ACM SIGKDD international conference on knowledge discovery & data mining*. 1269–1278.
- [22] Jundong Li, Harsh Dani, Xia Hu, and Huan Liu. 2017. Radar: Residual analysis for anomaly detection in attributed networks.. In *IJCAI*, Vol. 17. 2152–2158.
- [23] Yuening Li, Xiao Huang, Jundong Li, Mengnan Du, and Na Zou. 2019. Specae: Spectral autoencoder for anomaly detection in attributed networks. In *Proceedings of the 28th ACM international conference on information and knowledge management*. 2233–2236.
- [24] Can Liu, Li Sun, Xiang Ao, Jinghua Feng, Qing He, and Hao Yang. 2021. Intention-aware heterogeneous graph attention networks for fraud transactions detection. In *Proceedings of the 27th ACM SIGKDD conference on knowledge discovery & data mining*. 3280–3288.
- [25] Jie Liu, Mengting He, Xuequn Shang, Jieming Shi, Bin Cui, and Hongzhi Yin. 2024. Bourne: Bootstrapped self-supervised learning framework for unified graph anomaly detection. In *2024 IEEE 40th International Conference on Data Engineering (ICDE)*. IEEE, 2820–2833.
- [26] Yang Liu, Xiang Ao, Zidi Qin, Jianfeng Chi, Jinghua Feng, Hao Yang, and Qing He. 2021. Pick and choose: a GNN-based imbalanced learning approach for fraud detection. In *Proceedings of the web conference 2021*. 3168–3177.
- [27] Yixin Liu, Kaize Ding, Qinghua Lu, Fuyi Li, Leo Yu Zhang, and Shirui Pan. 2024. Towards self-interpretable graph-level anomaly detection. *Advances in Neural Information Processing Systems* 36 (2024).
- [28] Yixin Liu, Zhao Li, Shirui Pan, Chen Gong, Chuan Zhou, and George Karypis. 2021. Anomaly detection on attributed networks via contrastive self-supervised learning. *IEEE transactions on neural networks and learning systems* 33, 6 (2021), 2378–2392.
- [29] Xuexiong Luo, Jia Wu, Amin Beheshti, Jian Yang, Xiankun Zhang, Yuan Wang, and Shan Xue. 2022. Comga: Community-aware attributed graph anomaly detection. In *Proceedings of the Fifteenth ACM International Conference on Web Search and Data Mining*. 657–665.
- [30] Xiaoxiao Ma, Jia Wu, Shan Xue, Jian Yang, Chuan Zhou, Quan Z Sheng, Hui Xiong, and Leman Akoglu. 2021. A comprehensive survey on graph anomaly detection with deep learning. *IEEE Transactions on Knowledge and Data Engineering* 35, 12 (2021), 12012–12038.
- [31] Erxue Min, Yu Rong, Yatao Bian, Tingyang Xu, Peilin Zhao, Junzhou Huang, and Sophia Ananiadou. 2022. Divide-and-conquer: Post-user interaction network for fake news detection on social media. In *Proceedings of the ACM web conference 2022*. 1148–1158.
- [32] Junjun Pan, Yixin Liu, Yizhen Zheng, and Shirui Pan. 2023. PREM: A Simple Yet Effective Approach for Node-Level Graph Anomaly Detection. In *2023 IEEE International Conference on Data Mining (ICDM)*. IEEE, 1253–1258.
- [33] Yulong Pei, Tianjin Huang, Werner van Ipenburg, and Mykola Pechenizkiy. 2022. ResGCN: attention-based deep residual modeling for anomaly detection on attributed networks. *Machine Learning* 111, 2 (2022), 519–541.
- [34] Hezhe Qiao and Guansong Pang. 2024. Truncated affinity maximization: One-class homophily modeling for graph anomaly detection. *Advances in Neural Information Processing Systems* 36 (2024).
- [35] Xubin Ren, Lianghao Xia, Yuhao Yang, Wei Wei, Tianle Wang, Xuheng Cai, and Chao Huang. 2024. Sslrec: A self-supervised learning framework for recommendation. In *Proceedings of the 17th ACM International Conference on Web Search and Data Mining*. 567–575.
- [36] Amit Roy, Juan Shu, Jia Li, Carl Yang, Olivier Elshocht, Jeroen Smeets, and Pan Li. 2024. Gad-nr: Graph anomaly detection via neighborhood reconstruction. In *Proceedings of the 17th ACM International Conference on Web Search and Data Mining*. 576–585.
- [37] Hui Tang, Xun Liang, Jun Wang, and Sensen Zhang. 2024. DualGAD: Dual-bootstrapped self-supervised learning for graph anomaly detection. *Information Sciences* 668 (2024), 120520.
- [38] Jianheng Tang, Jiajin Li, Ziqi Gao, and Jia Li. 2022. Rethinking graph neural networks for anomaly detection. In *International Conference on Machine Learning*. PMLR, 21076–21089.
- [39] Li Wang, Peipei Li, Kai Xiong, Jiashu Zhao, and Rui Lin. 2021. Modeling heterogeneous graph network on fraud detection: A community-based framework with attention mechanism. In *Proceedings of the 30th ACM international conference on information & knowledge management*. 1959–1968.
- [40] Ning Wang, Zheng Wang, Yongwen Gong, Zhenlin Huang, Zhenlin Huang, Xing Wen, and Haitao Zeng. 2023. Unsupervised Data Anomaly Detection Based on Graph Neural Network. In *The International Conference on Cyber Security Intelligence and Analytics*. Springer, 552–564.
- [41] Qizhou Wang, Guansong Pang, Mahsa Salehi, Wray Buntine, and Christopher Leckie. 2023. Cross-domain graph anomaly detection via anomaly-aware contrastive alignment. In *Proceedings of the AAAI Conference on Artificial Intelligence*, Vol. 37. 4676–4684.
- [42] Zhe Xie, Haowen Xu, Wenxiao Chen, Wanxue Li, Huai Jiang, Liangfei Su, Hanzhang Wang, and Dan Pei. 2023. Unsupervised anomaly detection on microservice traces through graph vae. In *Proceedings of the ACM Web Conference 2023*. 2874–2884.
- [43] Bo Xu, Jimpeng Wang, Zhehuan Zhao, Hongfei Lin, and Feng Xia. 2024. Unsupervised Anomaly Detection on Attributed Networks With Graph Contrastive Learning for Consumer Electronics Security. *IEEE Transactions on Consumer Electronics* (2024).
- [44] Shujie Yang, Binchi Zhang, Shangbin Feng, Zhanxuan Tan, Qinghua Zheng, Jun Zhou, and Minnan Luo. 2023. Ahead: A triple attention based heterogeneous

- graph anomaly detection approach. In *Chinese Intelligent Automation Conference*. Springer, 542–552.
- [45] Yang Yang, Yuhong Xu, Yizhou Sun, Yuxiao Dong, Fei Wu, and Yueting Zhuang. 2019. Mining fraudsters and fraudulent strategies in large-scale mobile social networks. *IEEE Transactions on Knowledge and Data Engineering* 33, 1 (2019), 169–179.
- [46] Fanghui Zhang, Shichao Kan, Damin Zhang, Yigang Cen, Linna Zhang, and Vladimir Mladenovic. 2023. A graph model-based multiscale feature fitting method for unsupervised anomaly detection. *Pattern Recognition* 138 (2023), 109373.
- [47] Jiaqiang Zhang, Senzhang Wang, and Songcan Chen. 2022. Reconstruction enhanced multi-view contrastive learning for anomaly detection on attributed networks. *arXiv preprint arXiv:2205.04816* (2022).
- [48] Jinghui Zhang, Zhengjia Xu, Dingyang Lv, Zhan Shi, Dian Shen, Jiahui Jin, and Fang Dong. 2024. DiG-In-GNN: Discriminative Feature Guided GNN-Based Fraud Detector against Inconsistencies in Multi-Relation Fraud Graph. In *Proceedings of the AAAI Conference on Artificial Intelligence*, Vol. 38. 9323–9331.
- [49] Yu Zheng, Ming Jin, Yixin Liu, Lianhua Chi, Khoa T Phan, and Yi-Ping Phoebe Chen. 2021. Generative and contrastive self-supervised learning for graph anomaly detection. *IEEE Transactions on Knowledge and Data Engineering* 35, 12 (2021), 12220–12233.

A Supplement

A.1 Detailed Dataset Description

Three datasets are adopted for evaluation:

- **Retail_Rocket (Retail for short)**. This is a benchmark dataset collected from the Retail_rocket recommendation system. In this dataset, interactive relations between users and items include page views (View), add-to-cart (Cart), and transactions (Buy).
- **Alibaba**. This dataset is collected from Alibaba, one of the largest e-commerce platforms in China. It contains three interactive relations between users and items, *i.e.*, page view (View), add to cart (Cart), and purchase (Buy).
- **Amazon**. This dataset is collected from Amazon, it contains three interactive relations among users: U-P-U links users reviewing at least one product, U-S-U links users having at least one identical star rating within a week, U-V-U links linguistically similar users.
- **YelpChi**. This dataset is collected from Yelp, it contains three interactive relations among users: R-U-R connects the reviews posted by the same user, R-S-R connects reviews that have the same identical star rating, R-T-R connects reviews that posted in the same term.

A.2 Baselines

We compare our UMGAD with the following 20 baselines, which can be deeply divided into three categories:

Traditional GAD Method:

- **Radar [22]**: It is a learning framework for characterizing the residuals of attribute information in anomaly detection and its consistency with network information.

Specific GAD Methods:

- **ComGA [29]**: It is a novel community-aware attribute graph anomaly detection framework that contains a customized deep graph convolutional network which is capable of improving the information dissemination mechanism of GNNs from the perspectives of community segmentation and community structure and feature learning.
- **TAM [34]**: It learns custom node embeddings for our anomaly measure by maximizing the local affinity of nodes with their neighbors. TAM is optimized on a truncated graph rather than the original graph, where non-homogeneous edges are iteratively removed to mitigate non-homogeneous edge (*i.e.*, edges connecting anomalous nodes to normal nodes) bias.

CL-based GAD Methods:

- **CoLA [28]**: It proposes a well-designed GNN-based contrastive learning model to learn the information embedding from high-dimensional attributes and local structures, which makes full use of the local information in the network data by designing a novel contrastive instance pair sampling method.
- **ANEMONE [18]**: It first utilizes a GNN backbone encoder with a multi-scale contrastive learning objective to capture the pattern distribution of graphs by simultaneously learning the consistency between segment and context-level instances; then a statistical

anomaly estimator is employed to assess the anomalies of each node from multiple perspectives based on the degree of consistency.

- **Sub-CR [47]**: It is a self-supervised learning framework that jointly optimizes two modules, multi-view comparison-based learning as well as attribute-based reconstruction, to more accurately detect anomalies on attribute networks.
- **ARISE [11]**: It is a novel framework for graph anomaly detection based on substructure-aware attribute networks. ARISE differs from previous algorithms by focusing on learning substructures in graphs to recognize anomalies.
- **SL-GAD [49]**: It constructs different contextual views based on the target nodes and uses two modules, Generative Attribute Regression and Multi-View Comparative Learning, for anomaly detection. The Generative Attribute Regression module allows for capturing attribute anomalies, while the Multi-View Comparative Learning module can utilize richer structural information from multiple views to capture structural anomalies as well as mixed structural and attribute anomalies.
- **PREM [32]**: It consists of two modules - a preprocessing module and an isochronous bit matching module - designed to eliminate the need for message-passing propagation during training and employs a simple contrastive loss, which reduces training time and memory usage.
- **GCCAD [2]**: It proposes a pre-training strategy to solve the label scarcity problem in anomaly detection. Inspired by the idea of context-aware comparison targeting, GCCAD suggests constructing pseudo anomalies by corrupting the original graph.
- **GRADATE [10]**: It is a multi-view multi-scale contrastive learning framework including node-subgraph contrastive learning and subgraph-subgraph contrastive learning, which can better capture the different features between normal and abnormal substructures and help to recognize complex structural anomalies.
- **VGOD [17]**: It is a variance-based graph outlier detection method that combines a variance-based model and an attribute reconstruction model to detect outliers in a balanced way.

GAE-based GAD Methods:

- **GCNAE [19]**: It is an unsupervised learning framework for graph-structured data based on a variational graph autoencoder, which uses GCN as an encoder, simple vector inner product as a decoder, and latent variables to learn interpretable potential representational embeddings of undirected graphs.
- **DOMINANT [8]**: It learns node embeddings by modeling graph topology and node attributes using GCN and uses the learned node embeddings to reconstruct the original data via a deep autoencoder, with good results.
- **AnomalyDAE [12]**: It is a deep joint representation learning framework for anomaly detection via dual self-encoders that captures complex interactions between network structure and node attributes to obtain high-quality network embeddings.
- **AdONE [1]**: It is a deep unsupervised autoencoder-based approach and incorporates adversarial learning to learn the structure of the network and attribute-based embedding separately in a coupled manner to minimize the impact of outliers.

- **GAD-NR [36]**: It combines neighborhood reconstruction for graph anomaly detection, aiming to reconstruct the entire neighborhood of a node based on the corresponding node representation, including the local structure, self-attributes, and neighbor attributes.
- **ADA-GAD [15]**: It is a novel two-stage anomaly denoising autoencoder framework. In the first stage, the denoising method generates graphs with reduced anomaly levels and trains a graph autoencoder on them. In the second stage, the decoder is discarded while the encoder is retained, and a new decoder is trained for detection on the original graph. Additionally, ADA-GAD introduces node anomaly distribution regularization to further prevent anomaly overfitting.
- **GADAM [3]**: It is a novel Local Inconsistency Mining (LIM) approach that resolves the conflict between LIM and GNN messaging and enhances anomaly detection through an improved message passing mechanism.
- **AnomMAN [4]**: It proposes a GCN-based framework for detecting anomalies on multi-view attribute networks called AnomMAN that considers attributes and various interactions on multi-view attribute networks and uses an attention mechanism to fuse the importance of all views.

A.3 Time Complexity Analysis

The proposed UMGAD consists of three critical components: original-view graph reconstruction, augmented-view graph reconstruction, and dual-view contrastive learning. In original-view graph reconstruction, the time complexity of GMAE is $O(|\mathcal{V}| \times L \times f)$, and the time complexity of attention aggregation operation is $O(|\mathcal{V}| \times d_h \times f \times R)$, where $|\mathcal{V}|$ denotes the number of nodes, and L represents the number of Simplified GCN layers, d_h and f denote the dimension of latent vectors and the size of node attribute, R is the number of relational subgraphs. The overall time complexity of original-view graph reconstruction is $O(|\mathcal{V}| \times f \times (L + d_h \times R))$. For augmented-view graph reconstruction, the overall time complexity is $O(|\mathcal{V}| \times f \times (L + d_h \times R))$. The time complexity for dual-view contrastive learning is $O(|\mathcal{V}| \times f^2 + |\mathcal{V}| \times f)$. Hence, the entire time complexity of the proposed UMGAD is $O(|\mathcal{V}| \times f \times (L + d_h \times R + f + 1))$.

Additionally, original-view graph reconstruction and augmented-view graph reconstruction can also be accelerated in a parallel manner.

A.4 Additional Experiments

A.4.1 Anomaly Score Threshold Selection for Unsupervised Anomaly Detection (Continued RQ1). The results of ranked anomaly scores on two datasets with injected anomalies are shown in Fig. 5. Compared with the other four best-performing baselines, the curve of our UMGAD can converge quickly (become stable) to a position closer to the actual number of anomalies in the Retail and Alibaba datasets.

A.4.2 Performance Comparison in the Ground Truth Leakage Scenario (RQ5). (RQ5) How does UMGAD perform compared to other GAD methods in the scenario of threshold selection with ground truth leakage?

In this experiment, following [4], we use the number of anomalies to determine anomaly score thresholds for all methods on each dataset. Experimental results are reported in Table 4.

From Table 4, we can see that even with the introduction of ground truth, our model still achieves the best performance, which proves that UMGAD can capture anomaly information and identify anomalous nodes more effectively.

For the traditional GAD method, Radar uses residual networks to learn node attributes and capture anomalies simply and effectively, it is not as effective in capturing anomalous features when facing complex network structures. For the specifically designed for improving message passing mechanism (Specific for short) GAD methods, TAM performs better than ComGA since it learns custom node embeddings for our anomaly measure by maximizing the local affinity of nodes with their neighbors, and attenuates the effect of non-homogeneity of connected edges between abnormal and normal nodes.

For the CL-based GAD methods, GRADATE, VGOD, and ARISE are the three most effective of all methods. All three methods consider the importance of anomalous structural subgraphs to the GAD problem and learn subgraph features through subgraph sampling strategies to capture structural anomalies that are not easily detected by other methods. For the GAE-based GAD methods, most of them are working on how to learn better features of anomalous nodes for better detection of anomalous nodes during attribute and structural feature reconstruction, the four most effective and representative of these are GADAM, AnomMAN, GAD-NR, and ADA-GAD. Among them, ADA-GAD learns anomalous node features by graph augmentation, GAD-NR incorporates neighborhood reconstruction for the GAD task, and GADAM utilizes improved GNN message passing to enhance anomaly detection performance. However, these methods cannot solve the GAD problem on multiplex heterogeneous graphs, and thus perform slightly worse than our UMGAD. In addition, AnomMAN distinguishes itself from other GAE models in that it is oriented to the multiplex heterogeneous graphs constructed from ordinary heterogeneous graphs, which is similar to the object of study of our UMGAD. The performance of AnomMAN is limited since it does not capture subgraph structural anomalies well.

A.4.3 The effect of weights α and β that balance the importance of attribute and structure reconstruction. In this subsection, we perform a sensitivity analysis on α and β , two important hyperparameters for balancing attribute and structure reconstructions in the original view and subgraph-level augmented view, respectively. Experimental results are shown in Fig. 6. We can observe that: (1) the performance of UMGAD decreases rapidly when α and β take smaller (< 0.2) and larger (> 0.8) values, which emphasizes the importance of balancing feature and structure reconstructions, and smaller or larger values of α and β break the balance of the two reconstructions, resulting in the failure to capture more adequate anomaly information and affecting the model performance. (2) As the values of α and β gradually increase, the AUC index of the model first rises and then slowly decreases, and for the four datasets, the model achieves the best performance when α is set to 0.5, 0.5, 0.6, and 0.5, and β is set to 0.4, 0.4, 0.3, and 0.3, respectively.

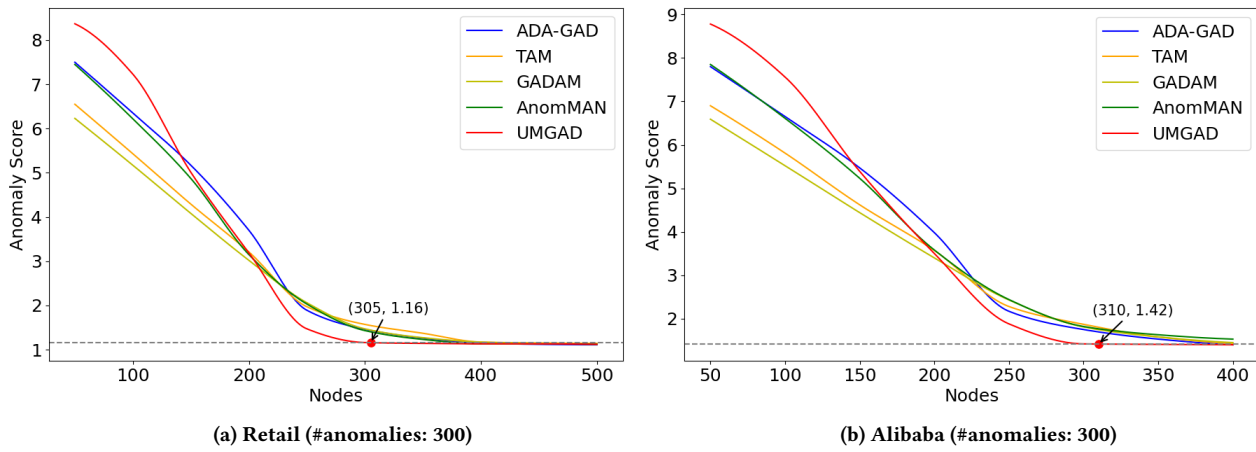


Figure 5: Visualization of ranked node anomaly scores for SOTA methods on two datasets with injected anomalies.

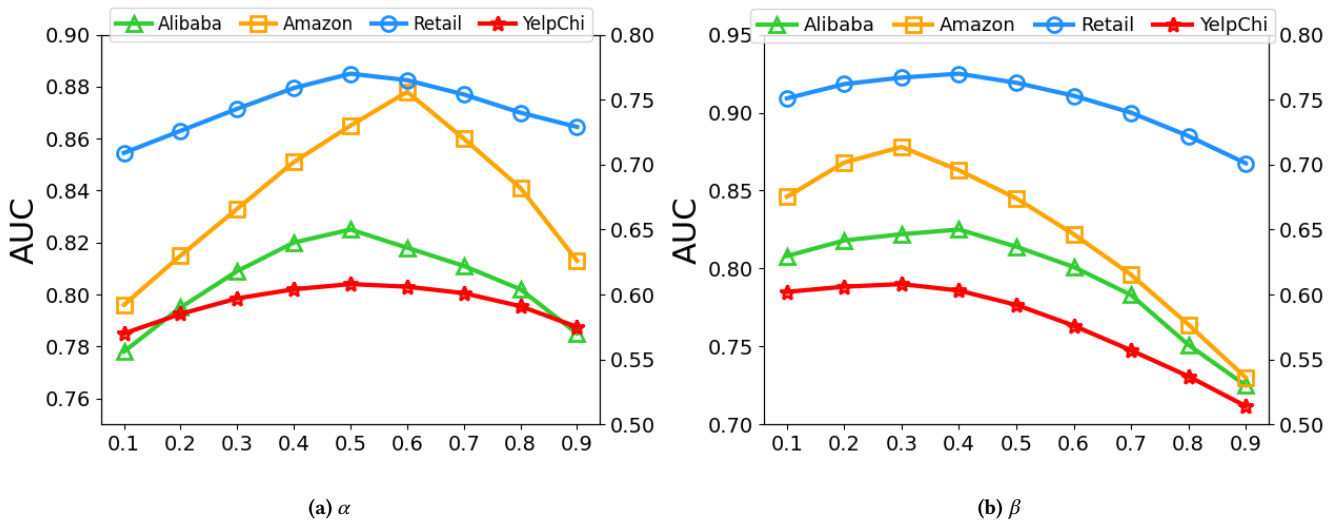


Figure 6: The effect of weights α and β in four datasets. The corresponding AUC values for the Alibaba and Amazon datasets are on the left Y-axis, and the corresponding AUC values for the Retail and YelpChi datasets are on the right Y-axis.

Table 4: Performance comparison of all models on four datasets in the scenario of threshold selection with ground truth leakage. Marker * indicates the results are statistically significant (t-test with p-value < 0.01).

Method		Retail		Alibaba		Amazon		YelpChi	
		AUC	macro-F1	AUC	macro-F1	AUC	macro-F1	AUC	macro-F1
Traditional	Radar	0.678	0.570	0.695	0.621	0.659	0.564	0.515	0.502
MPI	ComGA	0.725	0.667	0.778	0.672	0.725	0.642	0.553	0.504
	TAM	<u>0.753</u>	0.703	0.795	0.715	0.840	0.732	0.582	<u>0.554</u>
CL-based	CoLA	0.629	0.559	0.647	0.613	0.661	0.579	0.480	0.489
	ANEMONE	0.689	0.631	0.710	0.632	0.704	0.614	0.541	0.511
	Sub-CR	0.704	0.624	0.728	0.648	0.675	0.591	0.520	0.510
	ARISE	0.740	0.683	0.774	0.669	0.768	0.679	0.565	0.525
	SL-GAD	0.726	0.678	0.784	0.677	0.730	0.645	0.554	0.504
	PREM	0.724	0.675	0.782	0.670	0.735	0.649	0.557	0.513
	GCCAD	0.731	0.677	0.788	0.689	0.733	0.647	0.553	0.516
	GRADATE	0.746	0.686	0.790	0.705	0.805	0.719	0.574	0.544
	VGOD	0.745	0.679	0.791	0.703	0.797	0.707	0.571	0.531
GAE-based	DOMINANT	0.681	0.625	0.699	0.625	0.694	0.605	0.539	0.509
	GCNAE	0.683	0.633	0.701	0.631	0.679	0.591	0.541	0.511
	AnomalyDAE	0.679	0.622	0.697	0.626	0.708	0.610	0.545	0.515
	AdONE	0.685	0.624	0.707	0.637	0.721	0.634	0.556	0.526
	GAD-NR	0.749	0.691	0.789	0.710	0.829	0.721	0.579	0.550
	ADA-GAD	0.742	0.702	<u>0.796</u>	<u>0.716</u>	<u>0.841</u>	<u>0.732</u>	<u>0.582</u>	0.549
	GADAM	0.751	0.702	0.795	0.713	0.838	0.728	0.580	0.554
	AnomMAN	0.750	<u>0.703</u>	0.792	0.714	0.839	0.728	0.577	0.552
	UMGAD	0.780*	0.728*	0.831*	0.744*	0.886*	0.793*	0.612*	0.600*
<i>Improvement</i>		3.59% ↑	3.56% ↑	4.40% ↑	3.91% ↑	5.35% ↑	8.33% ↑	4.24% ↑	3.53% ↑